



Extended Second Law Analysis for Turboramjet Engines

Sara FAWAL^{1,*}, Ali KODAL²

¹ Department of Aeronautical Engineering, İstanbul Gelişim Üniversitesi, Cihangir Mah., Avcılar / İstanbul

² Department of Aeronautical Engineering, İstanbul Gelişim Üniversitesi, Cihangir Mah., Avcılar / İstanbul

ARTICLE INFO

2025, vol. 45, no.1, pp. 69-83
©2025 TIBTD Online.
doi: 10.47480/isibttd.1516527

Research Article

Received: 15 July 2024

Accepted: 14 December 2024

* Corresponding Author

e-mail: sfawal@gelisim.edu.tr

Keywords:

Brayton Cycle
TBCC Propulsion Performance
Maximum Power
EPLOS and PLOS

ORCID Numbers in author order:

0000-0002-2700-1682

0000-0001-7867-9672

ABSTRACT

Turbine based combined cycles (TBCC) monopolizes the benefits from the two different thermodynamic cycle configurations involved. The TBCC, which is based on an irreversible Brayton cycle, considered in this study is a wraparound configuration turboramjet engine. The turboramjet can be utilized in either turbojet (afterburner (AB) being ON or OFF), ramjet and even dual mode operation. However, for the dual mode operation the turbojet engine AB are considered to be ON. In addition, the ramjet thermodynamic assessment considers multi-oblique shock and single normal shock solution and Rayleigh flow calculation for the combustion chamber. The performance analysis and comparison for the turboramjet engine for dual mode operation is based on a maximum power approach under variations of Mach number and altitude. Moreover, the dual mode operation considered variations of inlet air mass flow; the split of air mass flow between the turbojet and ramjet. In addition, a brief comparison is provided of the turbojet while the afterburner is in ON or OFF mode utilizing the maximum power, EPLOS and PLOS optimization functions for variations of altitude and Mach number. Moreover, a component based evaluation under maximum power conditions for variation of Mach number is provided. The turbojet with an AB shows greater advantage at Mach number higher than unity as well as attaining maximum power outputs at minimum PLOS for lower compressor ratio parameters (θ_c). Whereas the turboramjet indicates that as the split of inlet air mass flow to the ramjet is increased beyond 50% the advantage in terms of η_{th} , η_o , f , TSFC, I_a , thrust and v_{NOZZLE} far supersede that of the turbojet with an AB.

Turboramjet Motorları için Genişletilmiş İkinci Yasa Analizi

MAKALE BİLGİSİ

Anahtar Kelimeler:

Brayton Çevrim
TBCC İtki Performans
Maximum Güç
EPLOS ve PLOS

ÖZET

Türbin tabanlı birleştirilmiş çevrimler (TBCC), iki farklı termodinamik çevrim konfigürasyonundan faydalarını tekelleştirir. Bu çalışmada ele alınan TBCC bir turboramjet motoru, tersinmez bir Brayton çevrimi sahiptir ve sarmalayıcı konfigürasyonludur. Turboramjet, turbojet (art yakıcı (AB) AÇIK veya KAPALI), ramjet ve hatta çift modlu çalışmada kullanılabilir. Ancak, çift modlu çalışma için turbojet motoru AB'nin AÇIK olduğu kabul edilir. Ek olarak, ramjet termodinamik değerlendirmesi, çoklu eğik şok ve tek normal şok çözümünü ve yanma odası için Rayleigh akış hesaplamasını dikkate alır. Çift modlu çalışma için turboramjet motorunun performans analizi ve karşılaştırması, Mach sayısı ve irtifa değişiklikleri altında maksimum güç yaklaşımına dayanmaktadır. Dahası, çift modlu çalışma, giriş hava kütlesi akışındaki değişiklikleri; hava kütlesi akışının turbojet ve ramjet arasında bölünmesini dikkate alır. Ek olarak, turbojetin, irtifa ve Mach sayısının değişimleri için maksimum güç, EPLOS ve PLOS optimizasyon fonksiyonlarını kullanarak, art yakıcı AÇIK veya KAPALI modundayken kısa bir karşılaştırması sağlanır. Ayrıca, Mach sayısının değişimi için maksimum güç koşulları altında bileşen tabanlı bir değerlendirme sağlanır. AB'li turbojet, daha düşük kompresör oranı parametreleri (θ_c) için minimum PLOS'ta maksimum güç çıkışlarına ulaşmanın yanı sıra birlikten yüksek Mach sayısında daha büyük avantaj gösterir. Turboramjet ise, ramjet'e giden giriş hava kütlesi akışının bölünmesi %50'nin üzerine çıktıkça, η_{th} , η_o , f , TSFC, I_a , itki ve v_{NOZZLE} açısından avantajın AB'li turbojetin çok ötesine geçtiğini gösterir.

NOMENCLATURE

AB	AB Afterburner
ALT	Altitude (km)
EPLOS	Effective Power Loss Parameter
MP	Maximum power (kW)
F_s	Specific Thrust (N-s/kg)
I_a	Air Specific Impulse (s)
\dot{m}_a	Inlet Mass flow of air (kg/s)
\dot{m}_{fb}	Fuel Mass flow of Burner (kg/s)
\dot{m}_{fAB}	Fuel Mass flow of Afterburner (kg/s)
PLOS	Power Loss Parameter
Q_R	Fuel Heating Value (kJ/kg)
\dot{Q}_{HT}	Total Heat Transfer (kJ/s)
\dot{Q}_{LT}	Total Heat Rejection (kJ/s)
\dot{Q}_{LK}	Rate of Heat Leak (kJ/s)
ST	Specific Thrust (N-s/kg)
TBCC	Turbine Based Combined Cycle
TSFC	Thrust Specific Fuel Consumption (kg/N-s)

T_H	Temperature of Hot Reservoir (K)
T_L	Temperature of Cold Reservoir (K)
η_b	Burner Efficiency
η_c	Compressor Efficiency
η_i	Intake/Diffuser Efficiency
η_j	Jet/Nozzle Efficiency
η_m	Mechanical Efficiency
η_p	Propulsive Efficiency
η_t	Turbine Efficiency
η_{th}	Thermal Efficiency
f_b	Fuel to Air Ratio of Burner
f_{ab}	Fuel to Air Ratio of Afterburner
f_r	Fuel to Air Ratio of Ramjet
θ_c	Compression Ratio Parameter
M_∞	Flight Mach Number
v_{NOZZLE}	Specific Volume (m ³ /kg)

INTRODUCTION

In terms of the ramjet, turbojet with afterburner and turbine based combined cycle (TBCC) engines, researchers have used the application of exergy exploration on various aspects in accordance to task requirements. (Şöhret et al. 2017) applied an exergy efficiency analysis for a ramjet engine using hydrogen fuel on a component (inlet, combustion zone and nozzle) and overall engine level. (Latypov 2009) conducted an exergy investigation based on various energy supplies to the air flow of the ramjet duct. (Latypov 2013) also assessed the specific impulse and thrust-economic characteristics of the ramjet using exergy analysis. (Ayaz and Altuntaş 2017) used exergy analysis on a generic ramjet engine under three different Mach regimes. (Moorhouse 2003) expanded the exergy method to the design of a complete aircraft vehicle based on mission requirements including component level evaluation. (Moorhouse and Suchomel C. F. 2001) further expands his study to the application of hypersonic vehicle design as an energy problem. (Moorhouse et al. 2002) also applied the exergy concept to the hypersonic inlet flow problem to determine the optimal shock-on-lip position for off-nominal flight condition. (Marley and Riggins D. W. 2011) also made use of exergy evaluation for a combined ramjet and turbojet engine during transient manoeuvres as well as the wake region of the turbojet engine. (Ispir et al. 2020) used an exergy simulation based platform for the thermodynamic cycle and performance optimization of the STRATOFly MR3 aircraft vehicle in DMR mode, ATR combustor, regenerator, nozzle, turbomachinery components and air turbo rocket bypass line. (Ehtaei et al. 2013) utilized an exergy approach for a turbojet engine with an afterburner (J85-GE-21) on a component level where the highest exergy efficiency was observed for the compressor and nozzle. (Roth and Marvis 2000) considered the loss management method for the analysis and quantification of technology impact of the F-5E/J85-GE-21 engine/airframe combinations and its relation to vehicle mass properties (weight). (Camberos and Moorhouse 2011) have published a book specifically describing the advantage of exergy analysis in the field of astronautics and aeronautics for various types of propulsion systems and even applying the concepts of exergy to airfoil drag evaluation. (Hayes et al. 2017) showed that exergy can

be adopted to various aspects in aerospace including design, performance and thermodynamic analysis of commercial aerospace systems, propulsion systems, aerodynamic and structural optimization, multi-disciplinary optimization based on the Breguet equation and mapping exergy over a variable flight envelope. (Riggins and Taylor 2006) also makes use of the laws of thermodynamics for the evaluation of a hyperspace vehicle applicable to both ramjets or scramjets using individual stream tubes as components within the overall fluid control volume. (Balli 2017) conducted a study of exergy destruction rates within engine components which were split into endogenous/exogenous and avoidable/unavoidable parts on a military turbojet engine with afterburner. (Balli 2017) then used the J85 turbojet engine with afterburner to assess the performance, exergetic, exergoeconomic, sustainability and environmental damage cost at Idle (ID), Intermediate (INT), Military (MIL) and Afterburner (AB) operation modes. (Balli 2014) further considered the afterburning effect on energetic and exergetic performance of an experimental Turbojet Engine (TJE) and to determine thermodynamic inefficiencies at military (MIL) and afterburner (AB) operation modes. (Akkaya et al. 2007) defined an exergetic performance coefficient (EPC) to assess a fuel cell power generation system (fuel cell stack, afterburner, fuel and air compressors, and heat exchangers) fed by hydrogen. (Yüksel et al. 2020) evaluated the exergetic analyses at Military (MIL) and Afterburner (AB) process modes of the (J85-GE-5H) military turbojet engine using kerosene (JP-8) and hydrogen (H₂) fuels. (Balli and Güneş 2017) conducted a performance assessment for both MIL and AB operation modes; and while under afterburner operation, examined energetic and exergetic performances and the effects on the environmental, ecological and sustainability metrics of the engine. (Akkaya et al. 2008) utilize an exergetic performance coefficient (EPC) for a gas turbine to investigate design parameters including fuel utilization, current density, recuperator effectiveness, compressor pressure ratio and pinch point temperature, to achieving higher exergy output with lower exergy loss in the system. (Bastani et al. 2015) applied exergy analysis and showed that the greatest exergy loss is in the afterburner due to its high irreversibility; therefore, the optimization of afterburner has an important role in reducing the exergy loss of total turbojet engine cycle.

(Yüksel et al. 2020) conducted an exergy-based economic and sustainability analysis for a (J85-GE-5H) military turbojet engine (TJE) using kerosene and H₂ fuel under MIL and AB regimes where higher exergy destruction occurred in the afterburner exhaust duct (ABED) and combustion chamber (CC) which led to higher exergy destruction costs. (Niknamian 2020) exergy analysis on J85-GE-21 turbojet engine and system optimization based on PSO (Particle Swarm Optimization) methods which showed that highest and lowest exergy efficiency of the engine components corresponded to the diffuser and compressor respectively. (Sürer and Arat 2018) performed a critical mini review exergy analyses of jet engines which concluded that if there is no afterburner, the combustion chamber has the greatest exergy destruction and thus minimum exergy efficiency due to its highly thermodynamically irreversible process; whereas the presence of an afterburner constitutes the biggest exergy destruction and smallest exergy efficiency. (Dong et al. 2018) revealed that the exergy analysis method can be used as a direct indication of the weaknesses of an entire energy system, reveal the interactions among system components and estimate the realistic work potential of different subsystems; it also provides a significant guidance for the improvement of engine performance, reduction of fuel consumption and optimization of engine combustion. (Noori et al. 2015) made use of four objective functions (F_s , TSFC, η_{th} and η_p) for the optimization of an ideal turbojet engine with afterburner. (Nasab and Ehyaei 2019) conducted an exergy analysis for the J85-GE-21 turbojet engine with afterburner where the highest exergy efficiency was demonstrated by the diffuser and the lowest belonged to the compressor. (Liu et al. 2023) performed a cycle optimization of a turboramjet to determine the optimal switch point in terms of both altitude and Mach number between the turbojet and ramjet. (Rajashankar et al. 2024) performed a switch point analysis for an engine component optimization of the turbojet for a set mass flow such that the desired thrust at the handover point to the ramjet is achieved. (Xi et al. 2023) investigated a thrust augmentation control schedule during mode transition of a turboramjet engine based on the air inlet, available airflow and the engine demand airflow. In latest developments, (Lockheed Martin 2024) is designing the successor of the TBCC wrap around type configuration SR-71 (maximum Mach 3.3) as an intelligence, surveillance and reconnaissance (ISR) hypersonic aircraft with an under over type configuration utilizing a turbine engine at low speeds and a scramjet engine at high speeds (maximum Mach 6); the successor aircraft is called the SR-72 and also denoted as the "Son of Blackbird" or "Darkstar".

It is clear that the use of exergy as an analysis tool provides an advantage in the evaluation and optimization of aircraft gas turbine propulsion systems. Identification of the level of exergy destruction can be made on a component level and subsequently exploit optimization functions for the improvement of TSFC, ST, η_{th} and η_p thus reducing the ecological impact of aircraft based engines on the environment.

This paper presents two case studies for various gas turbine engine configurations where the performance analysis and comparison takes a shift towards the more constraining parameters which are primarily Mach number and altitude. Case I begins with the performance evaluation on a maximum power basis between a turbojet with and without an AB, in addition to utilizing the PLOS and EPLOS optimization

functions as previously defined by (Fawal and Kodal 2019, 2021). Moreover, the size variation of individual engine components amongst both engine configurations was evaluated. Subsequently, Case II examines the performance of the TBCC turboramjet wraparound configuration was also evaluated on a maximum power basis for dual mode operation. In dual mode operation assessments were made for variations of altitude and inlet air mass flow; the split of air mass flow between the turbojet and ramjet. Note that in dual mode operation the turbojet engine AB are considered to be ON.

THEORETICAL REPRESENTATION

The basis of the turboramjet powerplant with an afterburner (AB) depends on the irreversible Brayton configuration and its T-s diagram are illustrated in Figure 1. The fundamental precept of this Brayton configuration has all the same processes as the turbojet with and without an AB and the ramjet. As previously stated the turboramjet engine with an AB operates amongst a heat source at high temperature, T_H , and a heat sink at low temperature, T_L . In the AB configuration there are two (\dot{Q}_{H1}) rates of heat transferred from the heat source to the turbojet engine; in the ramjet mode only one (\dot{Q}_{H2}) rate of heat is transferred from the high temperature source; however, there is still only one (\dot{Q}_L) rate of heat is dissipated to the heat sink from the turboramjet powerplant with an AB. Figure 1b also depicts the various engine thermodynamic cycle configurations: turbojet without an AB (**orange**); turbojet with an AB (**black**) and ramjet (**green**).

Similar to the turbojet with an AB and ramjet engines the performance analysis and comparison for the turboramjet engine also takes a transformation towards Mach number and altitude. Moreover, the **dual** mode operation was considered and assessed as variations of altitude and inlet air mass flow; the split of air mass flow between the turbojet and ramjet. Note that in dual mode operation the turbojet engine AB are considered to be ON. In addition, the performance evaluations have also been assessed under a maximum power regime for the turboramjet.

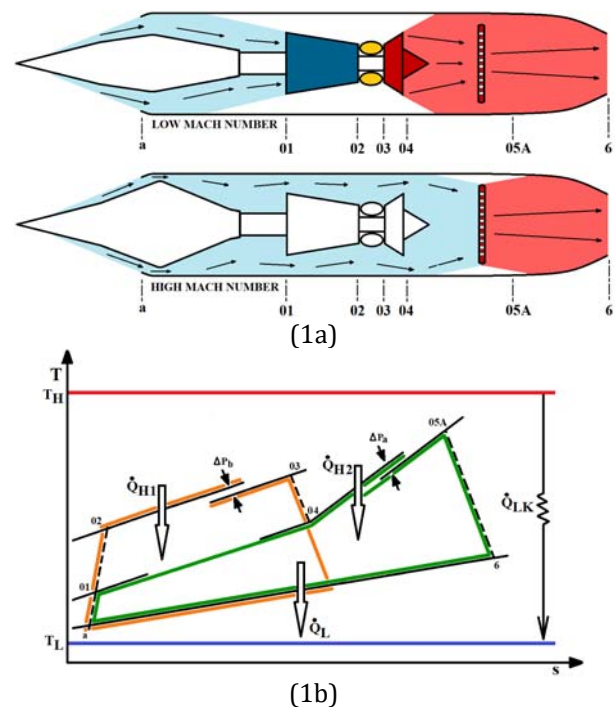


Figure 1. Engine arrangement (a) and T-s schematic representation of a turboramjet cycle (b) with an afterburner

Table 1 represents the combination of values taken for the turbojet with and without an AB as well as the values for the ramjet condition (the inlet area of the ramjet is now considered as 0.5m²); departures from these quantities are represented within the necessary figures. The essential propulsion equations for the powerplant state point computations may be obtained from (El-Sayed 2016).

Table 1. Delegated variable inputs for Turboramjet condition.

T _L = 200 K	η _j = 0.95	γ _g = 1.333
T _H = 2200 K	η _m = 0.99	R = 287 J/kg K
T _a = 223.3 K	η _b = 0.98	Di = 0.8 m
P _a = 26.5 kPa	C _{pa} = 1.005 kJ/kg K	Q _R = 43000 kJ/kg
ξ = 0.01	C _{pg} = 1.148 kJ/kg K	η _c = 0.87
η _i = 0.93	γ _a = 1.4	η _t = 0.9
M = 0.5	ΔP _b = 0.96	T ₀₃ = 1200 K
η _{ab} = 0.9	ΔP _{ab} = 0.97	T ₀₅ = 2000 K
δ = 12	A _i = 0.5 m ²	ALT = 10000 m

Case I: Turbojet with and without AB

The power generated by the turbojet powerplant configuration with an AB is defined as:

$$\dot{W} = \dot{Q}_{HT} - \dot{Q}_{LT} = \dot{Q}_H - \dot{Q}_L \quad (1)$$

The total heat dissipation rates from the high temperature reservoirs to the combustion chamber and the AB are given as:

$$\dot{Q}_{HT} = \dot{Q}_H + \dot{Q}_{LK} = \dot{m}_{fb}Q_R\eta_b + \dot{m}_{fab}Q_R\eta_{ab} + \dot{m}_a\xi C_{pa}(T_H - T_L) \quad (2)$$

Where $\dot{Q}_H = \dot{Q}_{H1} + \dot{Q}_{H2}$ which are the heat transfer rates from the combustion chamber and afterburner respectively.

Exergy destruction is defined as the reversible power, less the actual power of a cycle; where the reversible work is the power generated by the Carnot cycle and the actual power is given as the kinetic energy of the cycle and their formulation is given below:

$$\dot{X}_{DES} = \dot{W}_{rev} - \dot{W}$$

$$\dot{W}_{rev} = \dot{m}_f Q_R \eta_{Carnot}$$

$$\dot{W} = 0.5(1 + f)C_6^2 - C_a^2$$

Where η_{Carnot} is the Carnot efficiency

In addition, two supplementary cycle optimization functions are prescribed as power loss (PLOS) and effective power loss (EPLOS). Where PLOS is defined as the quotient between destroyed exergy and reversible power:

$$PLOS = \frac{\dot{X}_{DES}}{\dot{W}_{rev}} \quad (3)$$

EPLOS is designated as the ratio of ideal minus actual power of the Brayton cycle to the reversible power.

$$EPLOS = \frac{\dot{W}_{Brayn} - \dot{W}}{\dot{W}_{rev}} \quad (4)$$

$$\text{Where } \dot{W}_{Brayn} = \dot{Q}_{HT} \left[1 - \frac{1}{\theta_c} \right]$$

As (Fawal and Kodal 2019) prescribed, PLOS and EPLOS provide a better assessment of the performance and power losses throughout the operation of the engine cycle. The evaluation of

the turbojet with and without an AB using PLOS and EPLOS can be seen from Figure 5 for variations of compressor efficiency and Figure 6 for variations of Mach number.

The fuel used for the combustion chamber is assumed to be the same as for the AB, therefore, Q_R is still the fuel heat liberated per unit mass for both the combustion chamber and the AB, \dot{m}_{fb} is the fuel mass flow rate and η_b is the efficiency for the combustion chamber, \dot{m}_{fAB} is the fuel mass flow rate and η_{ab} is the efficiency for the AB.

Compression ratio parameter, θ_c is still given as before and taken to be: $\theta_c = (P_{02}/P_{01})^{(\gamma-1)/\gamma}$.

By applying an energy balance across the burner (combustion chamber) and the after burner the total fuel to air ratio, f_{TJ} is determined as:

$$f_{TJ} = f_b + f_{ab} = \frac{C_{pt}T_{03} - C_{pa}T_{02}}{Q_R\eta_b - C_{pt}T_{03}} + \frac{(1+f_b)C_{pt}(T_{05}-T_{04})}{\eta_{ab}Q_R - C_{pt}T_{05}} \quad (5)$$

The thermal efficiency of the turbojet cycle with an AB becomes:

$$\eta_{th} = \frac{\dot{W}}{\dot{Q}_{HT}} = \frac{\dot{W}}{\dot{m}_{fb}Q_R\eta_b + \dot{m}_{fab}Q_R\eta_{ab}} \quad (6)$$

The thrust equation is reobtained by applying integral momentum equation through the appropriate selection of the new control volume across the engine.

$$F_{TJ} = \dot{m}_{aTJ}[(1 + f_b + f_{ab})C_6 - C_a] + A_6(p_6 - p_a) \quad (7)$$

where C_6 is now the new exit velocity at the exhaust nozzle after the AB, C_a is the flight speed, A_6 is the exhaust nozzle exit cross section area and f_b and f_{ab} are the fuel to air mass flow rate ratio of the combustion chamber and AB respectively.

As before, by presuming perfect expansion and taking into account a per unit mass basis, the specific thrust is rewritten as:

$$F_{STJ} = (1 + f_b + f_{ab})C_6 - C_a \quad (8)$$

In addition to the numerical optimization procedures, the Mass Flow, Gas Generator Speed, Shaft Force, Altitude models and propulsion equations are still applicable to the turbojet with an AB.

Case II: Turboramjet in Dual Mode Operation

Equations (1) to (6) of the turbojet with an AB are still applicable when considering the turboramjet engine configuration. However, for the ramjet portion distinct considerations must be accounted for and provided in the formulations below.

The diffuser stagnation pressure ratio (ram recovery) for the ramjet is based on the (MIL-E-5007D 1973) specification and valid for Mach numbers between 1-5:

$$r_d = 1 \text{ For Mach Number } < 1 \quad (9)$$

$$r_d = 1 - 0.075(M_\infty - 1)^{1.35} \text{ From Mach } 1 \text{ to } 5 \quad (10)$$

$$r_d = 800/(M^4 + 938) \text{ For Mach Number } > 5 \quad (11)$$

The Mach number entering the afterburners is assumed not to exceed 0.25, thus ensuring subsonic burning conditions.

Implementing an energy balance at the inlet and exit of the afterburners and Rayleigh flow solutions based on tables and formulations of gas dynamics obtained from (Keith and John 2006) the fuel to air ratio, f_R for the ramjet is derived as:

$$f_R = \frac{C_{pa}(T_{04} - T_{0a})}{QR\eta_{ab} - C_{pa}T_{04}} \quad (12)$$

The mass flow for the ramjet engine is now defined from free stream conditions as:

$$\dot{m}_{aR} = \rho_a A_1 C_a \quad (13)$$

The total thrust generated by the turboramjet is considered as:

$$F = F_{TJ} + F_R = \dot{m}_{aTJ}[(1 + f_b + f_{ab})C_6 - C_a] + \dot{m}_{aR}[(1 + f_R)C_6 - C_a] \quad (14)$$

The specific thrust is also given as a total for the turboramjet as:

$$F_S = (F_{TJ} + F_R) / (\dot{m}_{aTJ} + \dot{m}_{aR}) \quad (15)$$

RESULTS AND DISCUSSION

The application of a turboramjet engine is to extract performance advantage from both Brayton configuration types: turbojet with AB and Ramjet utilizing an AB. As (Fawal and Kodal 2019, 2021) have exhaustively evaluated the turbojet without an AB, here, the provision of Case I was deemed necessary before progressing onwards to Case II. The disclosed Brayton cycle configurations in Case I and Case II are intended to highlight the advantages and limitations of the performance parameters and optimization functions of the respective powerplants.

Case I focuses on a maximum power assessment for variations of altitude and Mach number. Moreover, a component based comparison at maximum power for variations of Mach number at a given altitude is provided. In addition PLOS and EPLOS optimization functions for variations of compressor ratio parameter (θ_c) were evaluated.

Case II also evaluates the turboramjet on a maximum power basis for variations of Mach number, altitude and inlet air mass flow split.

Case I: Turbojet with and without AB

Figure 2 expresses the variations of thermal η_{th} (a), overall η_o (b) and propulsive η_p (c) efficiency for changes in altitude as a function of flight Mach number, M_∞ . For Mach numbers higher than unity the thermal efficiency of the turbojet with an AB becomes more advantageous at all altitudes; this is due to the much higher work / thrust output of the turbojet with an AB in comparison to the turbojet without an AB (see Figure 4). In addition, the thermal efficiency for a turbojet with an AB show an increase with increasing Mach number, whereas the turbojet without an AB show a slight decrease with increasing Mach number. On the other hand, the propulsive efficiency for a turbojet without an AB are about 20% higher for flight Mach numbers above 0.8 and at all altitudes than the turbojet with an AB; for Mach numbers below 0.8 the propulsive efficiency for a turbojet without an AB become about 10% higher than that of the turbojet with an AB, below Mach number of 0.4 the difference between the two configurations becomes increasingly

smaller. The overall efficiency for a turbojet without an AB still show greater advantage up to a Mach number of ~ 1.6 ; above this value the turbojet with an AB show a comparable advantage where the difference between the two engine configurations is around 5%. Figure 3 clearly shows that for a turbojet with an AB both the fuel to air ratio and TSFC are higher than that of a turbojet without an AB; this is an unavoidable consequence for the trade-off in increased thrust.

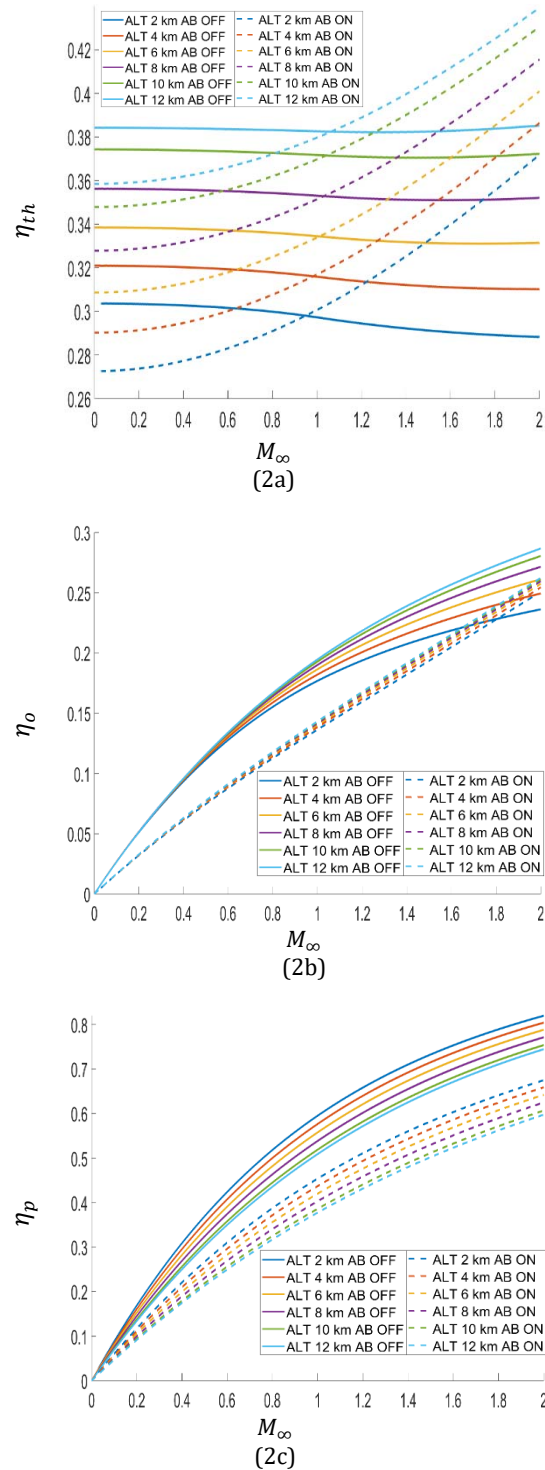


Figure 2. η_{th} , η_o and η_p efficiency for variations of altitude as a function of flight Mach number, M_∞ .

Figure 3 clearly shows that for a turbojet with an AB both the fuel to air ratio and TSFC are higher than that of a turbojet without an AB; this is an unavoidable consequence for the trade-off in increased thrust.

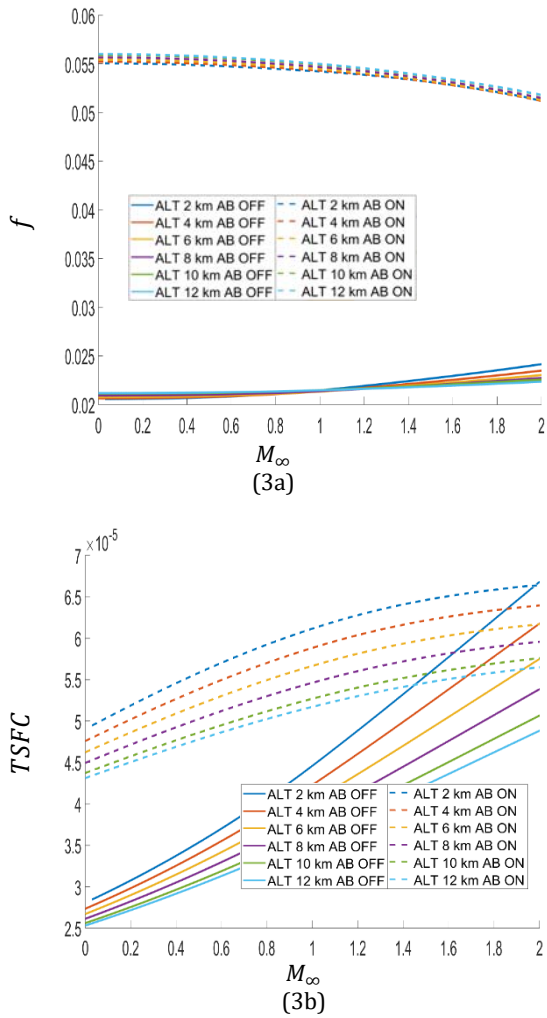


Figure 3. f and $TSFC$ efficiency for distinct quantities of altitude for variations M_∞ .

It is important to keep in mind that the purpose of using a turbojet with an AB is the significant increase in thrust, power and impulse of the system at all altitudes and flight Mach numbers (Figure 4). However, this comes at the expenditure for higher fuel consumption and heavier weight due to the increase in exhaust nozzle specific volume (Figure 4d). For altitudes higher than 6 km the thrust and power of both engine configurations intersect at a point. For example at an altitude of 12 km the red dot on Figure 4b corresponds to the two red dots on Figure 4a; what is seen is that the turbojet with an AB can achieve the same thrust and power as the turbojet without an AB at a much lower Mach number (0.6 vs. 1.6 respectively).

As previously mentioned, the main objective of the turbojet with an AB is the higher power output of the system, this can be seen again from Figure 5 and Figure 6. From both figures it can be seen that the difference in effective power loss parameter (EPLoS) between both engine configurations is quite small $\sim 5\%$ at maximum power for both turbojets with and without an AB; in addition, as the Mach number is increased from 0.8 to 1 the difference in EPLoS decreases. Thus the compressor efficiency η_c has a greater influence on EPLoS than the Mach number; this can also be seen from the figures presented by (Fawal et al. 2019). Therefore, from an EPLoS perspective (ignoring the margin of power gain) there is no significant advantage as to which engine configuration is used.

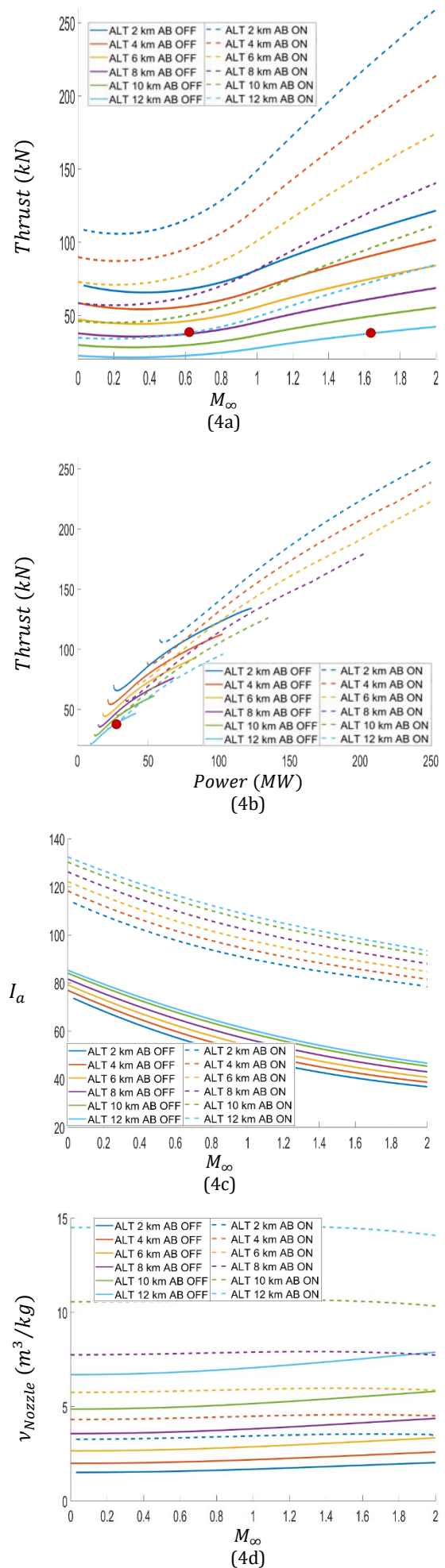


Figure 4. Thrust (a), I_a (c) and v_{Nozzle} (d) for variations of altitude as a function of M_∞ and Thrust (b) as a function of Power.

On the other hand, from PLOS point of view the, the exergy destruction of the turbojet with an AB is overall higher than a turbojet without an AB; at minimum PLOS 65% vs. 55% respectively. In addition, the difference at minimum PLOS between both engine configurations is about 10%. Moreover, for variations of compressor efficiency (Figure 5), at minimum PLOS for the turbojet with an AB occurs at the maximum power output ~ 34 MW and lower compressor ratio parameter $\theta_c \sim 2.62$, whereas the minimum PLOS for the turbojet without an AB is slightly shifted towards the right at lower power ~ 12 MW output and higher compressor ratio parameter $\theta_c \sim 2.88$, which means an increase in compressor size and inevitably weight.

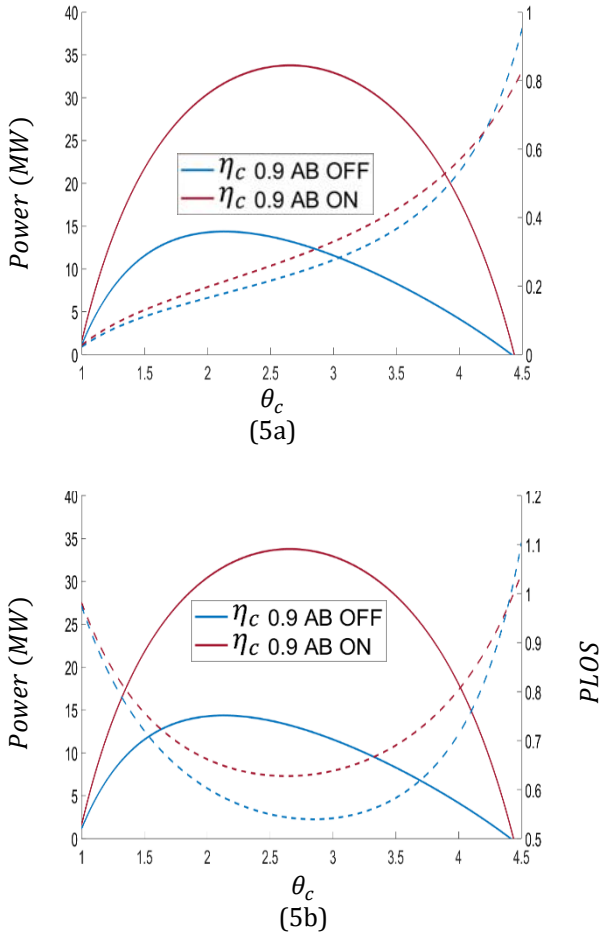


Figure 5. Power, EPLOS and PLOS for distinct quantities of η_c for variations of θ_c .

Furthermore, for variations of Mach number (Figure 6), at minimum PLOS the turbojet with an AB has a higher power output as Mach number increases at lower compressor pressure ratio: Mach 0.8, ~ 42 MW and $\theta_c \sim 2.47$ vs. Mach 1, ~ 52 MW and $\theta_c \sim 2.39$; whereas the turbojet without an AB, Mach 0.8, ~ 15 MW and $\theta_c \sim 2.65$ vs. Mach 1, ~ 18 MW and $\theta_c \sim 2.52$. Therefore, the turbojet with an AB displays an advantage of: lower θ_c and compressor weight and higher power output at the expense of higher exergy destruction. However, the turbojet with an AB having a lower θ_c and lower compressor weight needs to be compared to the increase in weight gain due to the AB components and exhaust nozzle.

From Figure 7, for a constant altitude of 10 km and changes in Mach number and as previously stated, that the overall dimension of the powerplant does not change while the respective powerplant constituents undergo size metamorphosis. For both engine configurations, at higher Mach numbers dimensions for diffuser increases, therefore, the selection of diffuser (ram recovery) develops as a crucial role

than at reduced Mach numbers. In addition, the exhaust nozzle for the turbojet with an AB is on average $\sim 85\%$ larger than that of the turbojet without an AB, which inevitably corresponds to an increase in engine weight. Therefore, a comparative and trade-off study of the decrease in θ_c and thus compressor weight, the $\sim 85\%$ increase in exhaust nozzle specific volume and the AB fuel components need to be examined.

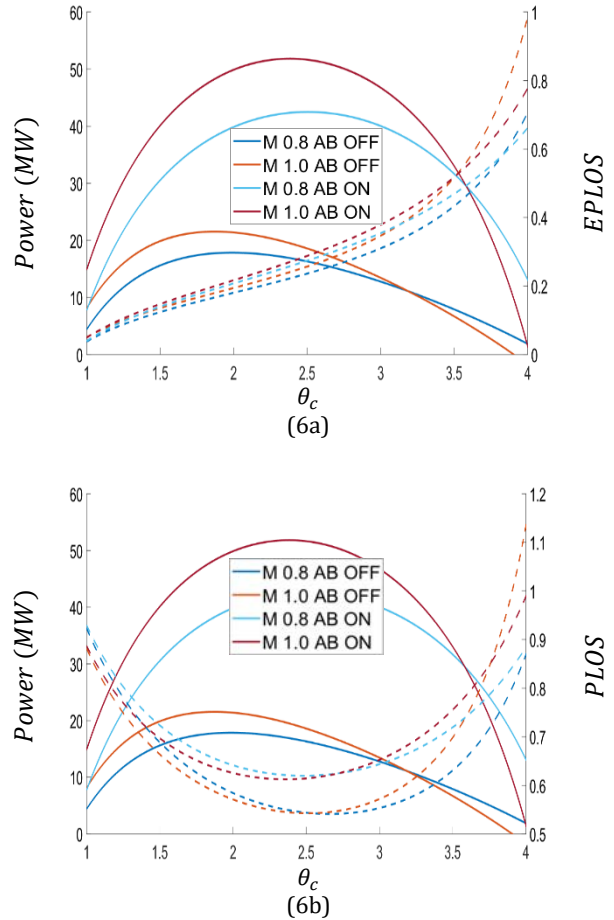
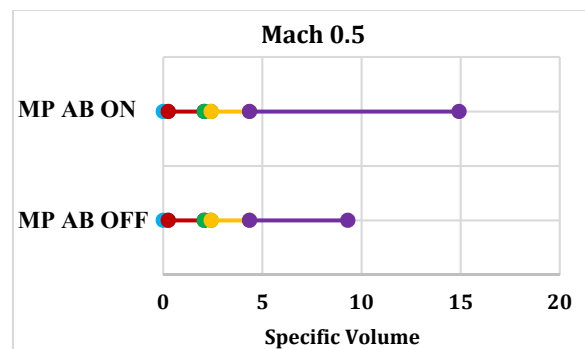
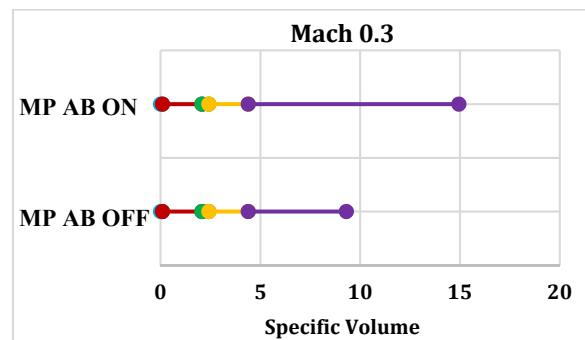


Figure 6. Power, EPLOS and PLOS for distinct quantities of M_∞ as a function of θ_c .

● Diffuser ● Compressor ● Burner ● Turbine ● Nozzle



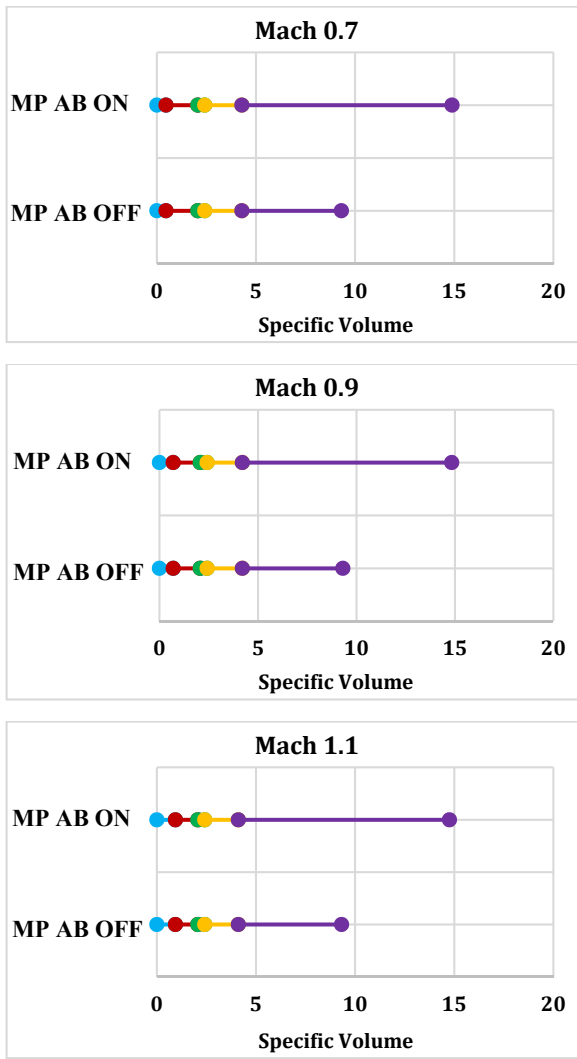


Figure 7. Dimensional metamorphoses of respective engine modules at maximum MP for variations M_∞ .

Case II: Turboramjet in Dual Mode Operation

Figure 8 to Figure 10 is an altitude assessment of the turboramjet in dual mode operation at maximum power for variations of Mach number for a 25% to 75% inlet air mass flow split between the turbojet and ramjet respectively. The performance parameters of: thermal, propulsive and overall efficiency; fuel to air ratio, TSFC, impulse, thrust, power and specific volume were evaluated.

Figure 8 distinctly shows the limitation of turbojet operation as a function of altitude and Mach number. The maximum feasible operating range in terms of Mach number at an altitude of 2 km, 4 km, 6 km, 8 km, 10 km and 12 km to 20 km are 1.97, 2.08, 2.19, 2.31, 2.44 and 2.51 respectively, after which a divergence in the propulsion solutions are encountered. The propulsive efficiency of the turbojet still outweighs the use of the ramjet up to a Mach number of 2.5. However, falls short in terms of thermal and overall efficiency in the overlapping region of Mach 1.97 and 2.51. In terms of overall efficiency, the ramjet indicates highest performance at 3.36, 3.55, 3.74, 3.94, 4.15, 4.34, 4.47, 4.63, 4.73 and 4.89 Mach with 0.52, 0.54, 0.56, 0.58, 0.60, 0.63, 0.65, 0.68, 0.70 and 0.73 overall efficiencies for each altitude from 2 km to 20 km respectively. Whereas the turbojet reaches its maximum performance capability at 1.97, 2.08, 2.19, 2.31, 2.44 and 2.51 Mach with 0.25, 0.26, 0.28, 0.30, 0.31 and 0.32 overall efficiencies respectively for each altitude from 2 km to 12 km; note that beyond 12 km the overall efficiency

and Mach number remains the same. The thermal efficiency of the ramjet depicts a gradual decrease and takes a sharp decline beyond a Mach number of 4; thus, at 4.09, 4.24, 4.41, 4.6, 4.76, 4.9, 5.03, 5.16, 5.26, and 5.38 Mach with 0.48, 0.51, 0.54, 0.56, 0.60, 0.62, 0.64, 0.66, 0.68 and 0.70 thermal efficiencies are achieved. Whereas the turbojet reaches its maximum performance capability at 1.97, 2.08, 2.19, 2.31, 2.44 and 2.51 Mach with 0.37, 0.39, 0.42, 0.44, 0.46 and 0.48 thermal efficiencies respectively for each altitude from 2 km to 12 km; similarly, beyond 12 km the thermal efficiency and Mach number remains the same. The propulsive efficiency of the ramjet is nearly linear and illustrates an upper saturation limit for 2 km and 20 km at Mach numbers of 4.27, 4.45, 4.65, 4.85, 5.07, 5.22, 5.3, 5.37, 5.44 and 5.5 respectively; in addition, at a Mach number of 2 the propulsive efficiency decreases from 0.59 to 0.50 as the altitude increases from 2 km to 20 km. Whereas the turbojet reaches its maximum performance capability at 1.97, 2.08, 2.19, 2.31, 2.44 and 2.51 Mach with 0.67 propulsive efficiency respectively for each altitude from 2 km to 20 km; also the Mach number and propulsive efficiency does not change beyond 12 km.

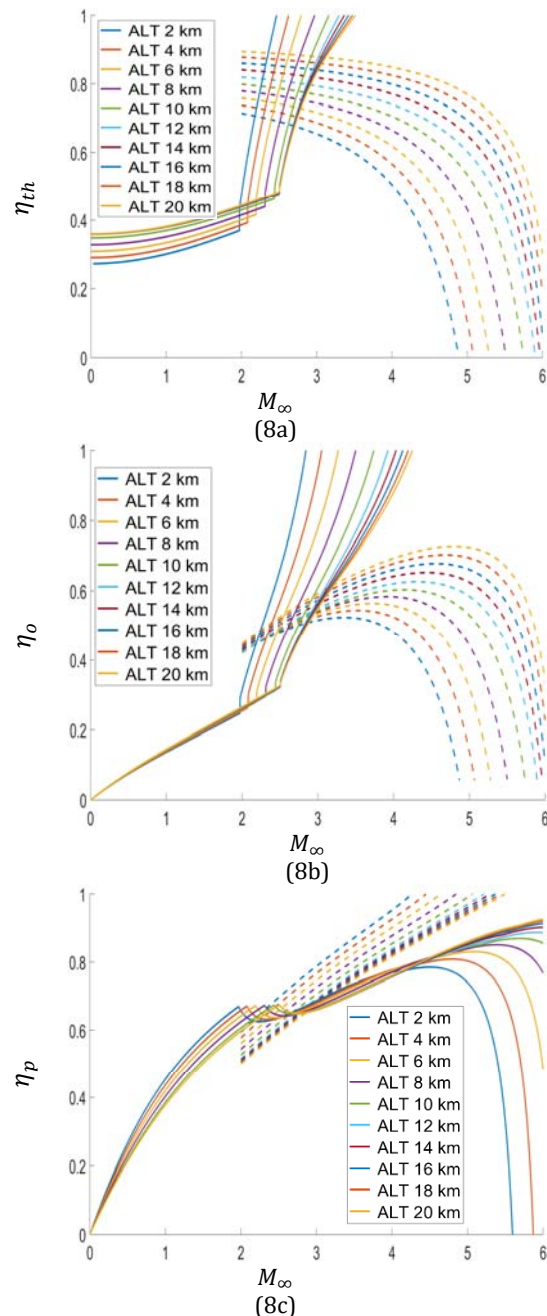


Figure 8. η_{th} , η_o and η_p for variations of altitude for turboramjet engine as a function of M_∞ .

Figure 9 shows the f , $TSFC$ (kg/N-s) and I_a (s) of the dual mode operating system. For all altitudes the ramjet indicates lower f and $TSFC$ and higher I_a than the turbojet. The minimum attainable f for the turbojet ranges from 0.05137, 0.0508, 0.05033, 0.04993 and 0.04861 for the previously specified Mach numbers and altitudes; in addition to showing a decrease in f for increasing altitude. On the other hand, the ramjet experiences an increase in f as the altitude increases. Nevertheless, at a Mach number of 2 the f increases from 0.04122 to 0.0441 which is still much lower than the f of the turbojet. Evidently this is due to the turbojet fuel contribution stemming from both the combustion chamber and afterburner, whereas the ramjet only utilizes the afterburner fuel for thrust generation. In addition, the ramjet exhibits a much greater advantage of attaining higher Mach numbers for even lower values of fuel to air ratio; i.e. as the Mach number increases the f also decreases. The turbojet reaches a maximum TSFC capability at 1.97, 2.08, 2.19, 2.31, 2.44 and 2.51 Mach with $6.637e-05$, $6.415 e-05$, $6.215 e-05$, $6.032 e-05$, $5.865 e-05$ and $5.694 e-05$ TSFC respectively for each altitude from 2 km to 12 km; in addition to a decrease in TSFC with increasing altitude notwithstanding that the Mach number and TSFC do not change beyond 12 km. For a TSFC of $5.694 e-05$, the operating range for the ramjet in term of Mach numbers are: 3.46, 3.67, 3.9, 4.14, 4.4, 4.62, 4.79, 4.96, 5.11 and 5.26 for altitudes from 2 km to 20 km respectively; where beyond a TSFC of $5.694 e-05$ operation becomes unrealistic.

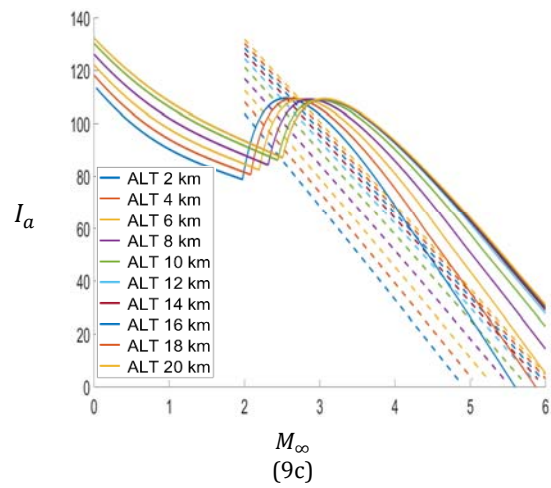
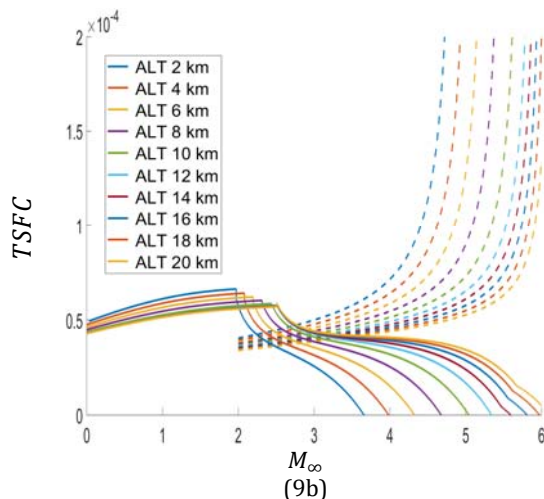
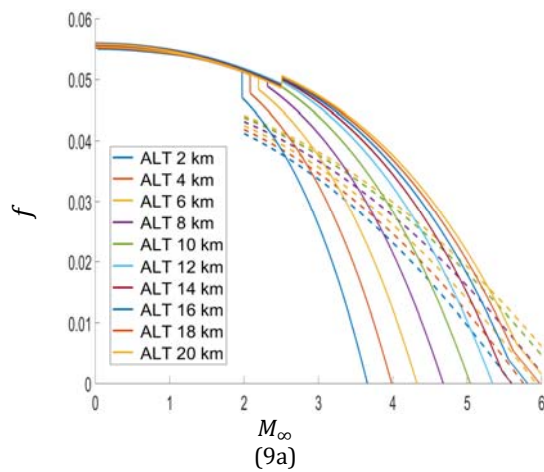
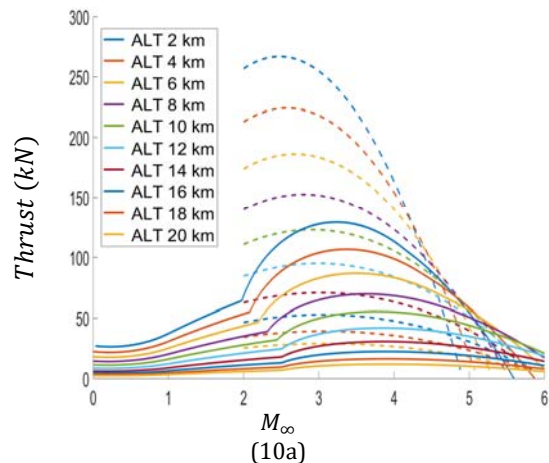


Figure 9. f , $TSFC$ and I_a for variations of altitude for turboramjet engine as a function of M_∞ .

Figure 10 depicts the thrust (kN) for variations of Mach number and power and the exit nozzle specific volume (m^3/kg) for variations of Mach number. In terms of thrust the turbojet is capable of achieving 64, 55, 47, 39, 32, 25, 18, 13, 10 and 7 kN of thrust at Mach numbers of 1.97, 2.08, 2.19, 2.31, 2.44, and 2.51 respectively for each altitude from 2 km to 20 km. Whereas the ramjet can produce 257, 213, 174, 140, 111, 85, 63, 47, 34 and 25 kN of thrust at a Mach number of 2 for each altitude from 2 km to 20 km. As expected, the thrust and power of the dual system decreases with altitude. Nonetheless, the ramjet is still capable of producing 7 kN of thrust at a Mach number of 5.73. When examining the specific volume, the ramjet has a lower exit nozzle specific volume than the turbojet at all altitudes. For the turbojet, specific volumes of 3.5, 4.5, 5.8, 7.5, 9.9, 13.3, 18.3, 25, 34.3 and 46.9 are achieved at Mach numbers of 1.97, 2.08, 2.19, 2.31, 2.44, and 2.51 respectively for each altitude from 2 km to 20 km. Whereas the ramjet experiences limitations in specific volumes of 2.4, 2.9, 3.6, 4.5, 5.7, 7.3, 9.4, 12.0, 15.4 and 19.8 for operable Mach number maximums of 4.87, 5.07, 5.28, 5.5, 5.73, 5.89, 5.95 and 6 as the altitude increases from 2 km to 20 km. Moreover, as the altitude increases the specific volume of the turbojet becomes far too large for efficient operation and therefore too heavy. Altitudes at and above 10 km show approximately twice the increase in specific volume for the turbojet than the ramjet. Therefore, the turbojet can be used up to an altitude of 8 km and then completely switch to ramjet operation for altitudes of 10 km and beyond. Where at 20 km the specific volume of the ramjet is ~ 20 (which is obtained at 14 km for the turbojet) and ~ 47 for the turbojet respectively.



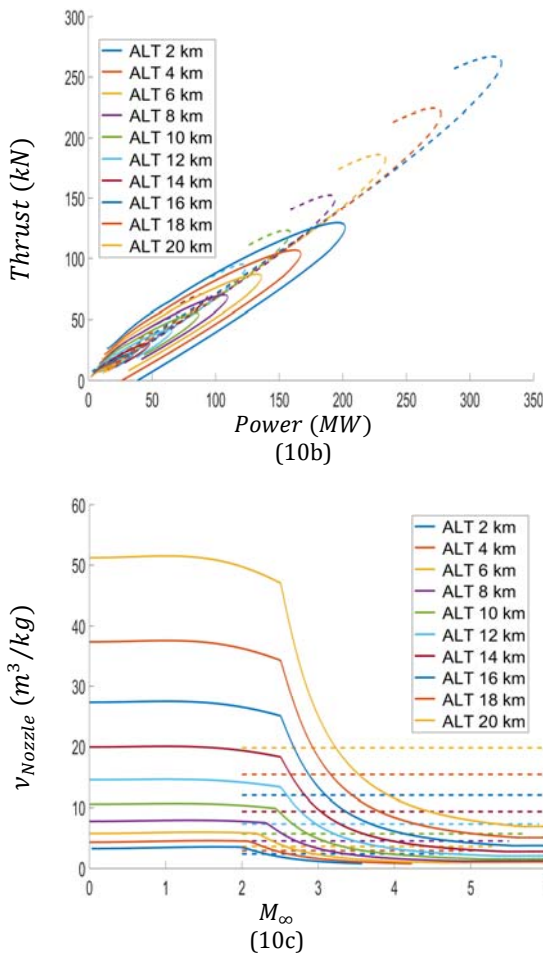


Figure 10. Thrust (a) and v_{Nozzle} (c) as a function of M_∞ and Thrust vs. Power for variations in altitude.

Figure 11 to Figure 19 is an assessment of variations of inlet air mass flow split between the turbojet and ramjet as a function of Mach number at 10 km and 20 km (all figures on the right and left respectively). The legend in these figures indicates the percentage of air mass flow being diverted to the ramjet (--dashed lines) and the remaining percentage being directed to the turbojet (--solid lines). It is also to note that curves of the same colour are complementary to each other; for example, the blue curves imply a 25% to 75% inlet air mass flow split between the ramjet and turbojet respectively. However, the exception to the previous statement are the purple curves, where 100% inlet air mass flow to the ramjet means 0% to the turbojet and vice versa. In addition, this part of the analysis has restricted the operation of the turbojet up to a Mach number of 2.5; as has previously mentioned the limitation of the turbojet application reaches a maximum operable Mach number of 2.4 for both altitudes of 10 km and 20 km respectively. Whereas, the constraint for the discussion of the ramjet analysis will be kept to a maximum Mach number of 4.4 and 5.26 for the altitudes of 10 km and 20 km respectively; this is due to the feasibility in terms of *TSFC* as stated previously. Also to note, the pressure and temperature at 10 km vs. 20 km are: 26.43 kPa and 223.15 K vs. 5.47 kPa and 216.65 K respectively.

Figure 11 and Figure 12 show that at 25% inlet air mass flow the turbojet is economically more effective in terms of both thermal and overall efficiency respectively at Mach 2. As the split of mass flow to the ramjet is increased (50% to 100%) it becomes quite distinct that the ramjet is much more beneficial. Also, in general, as the inlet mass flow of either system increases, so do the thermal and overall efficiencies. For the altitudes of 10 km and 20 km the maximum attainable thermal

efficiencies are: 0.23, 0.34, 0.41 and 0.46 versus 0.24, 0.36, 0.43 and 0.47 respectively. Whereas the ramjet thermal efficiencies are: 0.19, 0.35, 0.5 and 0.66 versus 0.21, 0.38, 0.56 and 0.73 at 10 km and 20 km respectively. In terms of overall efficiency, the turbojet achieves 0.16, 0.23, 0.27 and 0.3 versus 0.16, 0.24, 0.28 and 0.31 at 10 km and 20 km respectively. Whereas the ramjet overall efficiencies are: 0.19, 0.33, 0.46 and 0.6 versus 0.23, 0.39, 0.55 and 0.7 at 10 km and 20 km respectively. Note however, that the maximum overall efficiency (same as previous values) for the ramjet at 10 km are achievable at slightly lower Mach numbers: 4.35, 4.26, 4.2 and 4.17 for increases of inlet air mass flow split. Similarly, at 20 km the maximum overall efficiency for the ramjet are attained at: 5.07, 4.95, 4.88 and 4.82 Mach numbers for increasing mass flow split; in addition, for 50% to 75% air flow split the overall efficiency increases by 1% and at a 100% air flow split the overall efficiency increases by 3%.

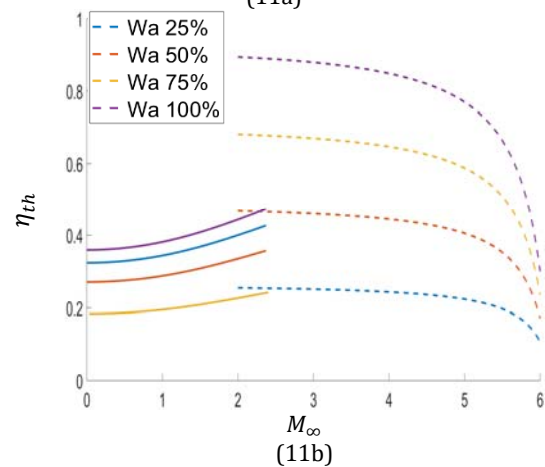
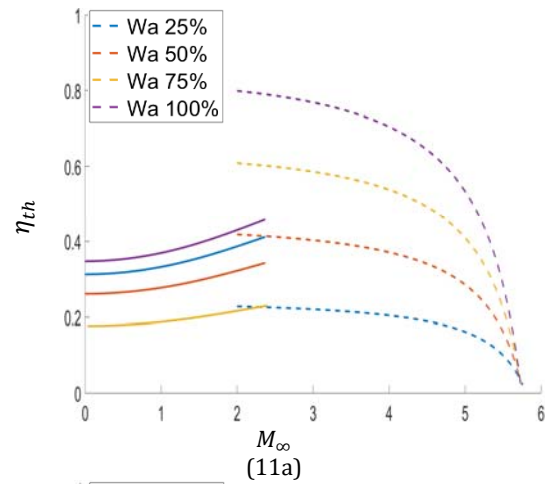
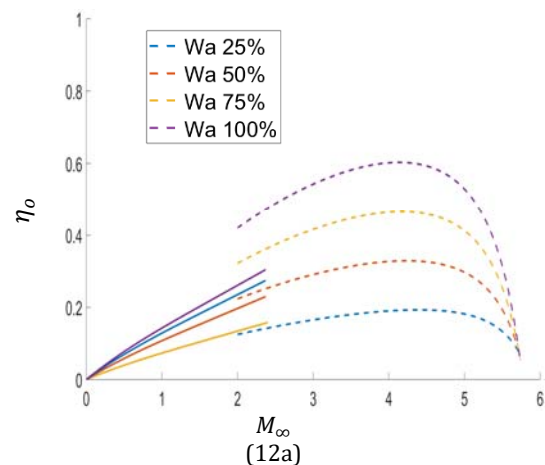


Figure 11. η_{th} for variations of inlet air mass flow at 10 km (a) and 20 km (b) for turbo-ramjet engine as a function of M_∞ .



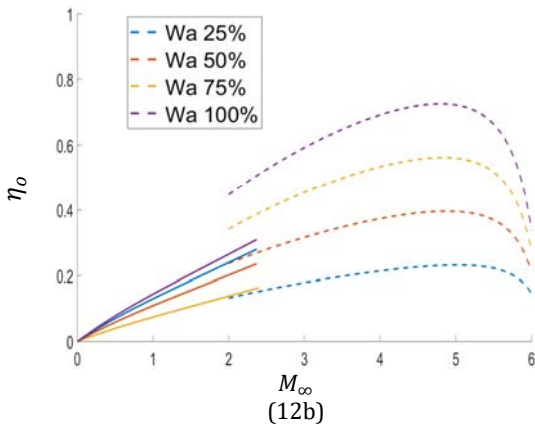


Figure 12. η_0 for variations of inlet air mass flow at 10 km (a) and 20 km (b) for turboramjet engine as a function of M_∞ .

On the other hand Figure 13 indicates a better propulsive efficiency for the turbojet over the ramjet at all inlet air mass flow splits up to Mach 2. Beyond a Mach number of 2 the ramjet takes over and has a dominating effect on system performance. However, unlike the thermal and propulsive efficiency, the propulsive efficiency decreases as the inlet air mass flow to either system increases. This is due to the kinetic energy added to the air mass flow through the engine being higher than the propulsive power generated by the fully expanded exhaust jet. For the turbojet, the attainable propulsive efficiencies are: 0.69, 0.67, 0.67 and 0.66 versus 0.68, 0.66, 0.66 and 0.657 at 10 km and 20 km respectively. Whereas the ramjet propulsive efficiencies are: 1, 0.94, 0.92 and 0.91 versus 1, 1, 0.99 and 0.97 at 10 km and 20 km respectively; however, at 20 km and for 25% and 50% inlet air mass flow split the maximum propulsive efficiency is reached at 4.77 and 5.18 Mach respectively.

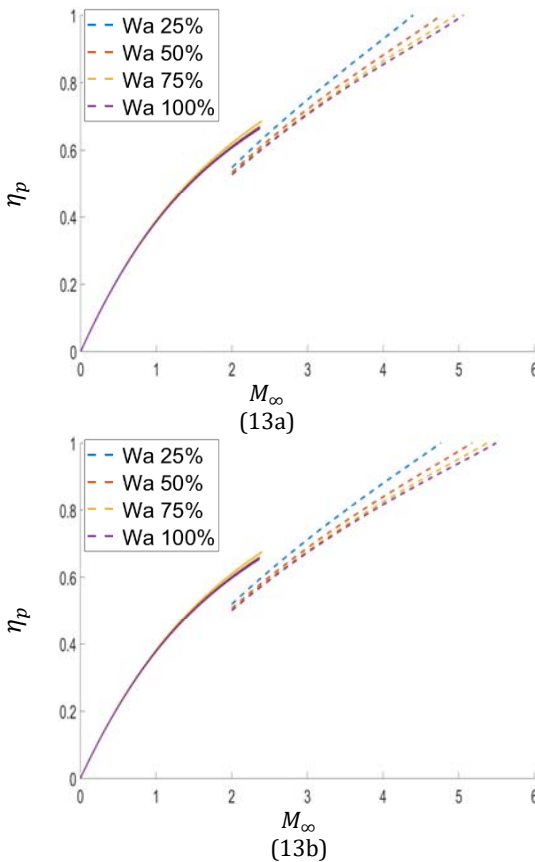


Figure 13. η_p for variations of inlet air mass at 10 km (a) and 20 km (b) flow for turboramjet engine as a function of M_∞ .

What is also interesting to note from Figure 11 to Figure 13 is that the variations on thermal overall and propulsive efficiency for the turbojet show slight variations from 10 km to 20 km,

whereas for the ramjet the changes are more pronounced. This effect is a direct result of the much higher attainable Mach numbers for the ramjet vs. the turbojet.

From Figure 14 and Figure 15 it is seen that the both the f and TSFC of either system decreases as the inlet air mass flow is increased. For a constant input of fuel this is an expected result. However, what is interesting to see is that the ramjet is not competitive enough with the turbojet until 75% inlet air mass flow is reached; below 75% (25% and 50%) the turbojet experiences lower f and TSFC. In addition, notwithstanding the changes of inlet air mass flow, the small change in temperature from 10 km 223 K to 20 km 216K has very little impact on the variation of f , which is completely independent of the free stream pressure and strongly dependent on the maximum temperature of the cycle; this effect is also observed on TSFC. For the turbojet the attainable f are: 0.103, 0.067, 0.056 and 0.05 versus 0.01, 0.066, 0.055 and 0.049 at 10 km and 20 km respectively. Whereas the ramjet f are: 0.1, 0.05, 0.033 and 0.025 versus 0.064, 0.032, 0.021 and 0.016 at 10 km and 20 km respectively. Here, we also see that the difference in altitude for the turbojet has very little impact on the f , whereas the ramjet experiences a significant decrease on f for an increase in altitude from 10 km to 20 km. When examining TSFC, the turbojet attains values of: 1.11e-04, 7.64e-05, 6.45e-05 and 5.85e-05 versus 1.06e-04, 7.34e-05, 6.23e-05 and 5.67e-05 at altitudes of 10 km and 20 km respectively. Whereas the ramjet TSFC values are: 1.76e-04, 1.04e-04, 7.36e-05 and 5.70e-05 versus 1.74e-04, 1.03e-04, 7.33e-05 and 5.69e-05 at 10 km and 20 km respectively. Interestingly, it is observed that for the turbojet the TSFC slightly decreases for an increase in altitude from 10 km to 20 km and therefore more fuel efficient, however, the ramjet values of TSFC are extremely close to each other. Therefore, with just an increase in altitude the ramjet remains static in terms of fuel efficiency to thrust output however has an advantage of a higher Mach number.

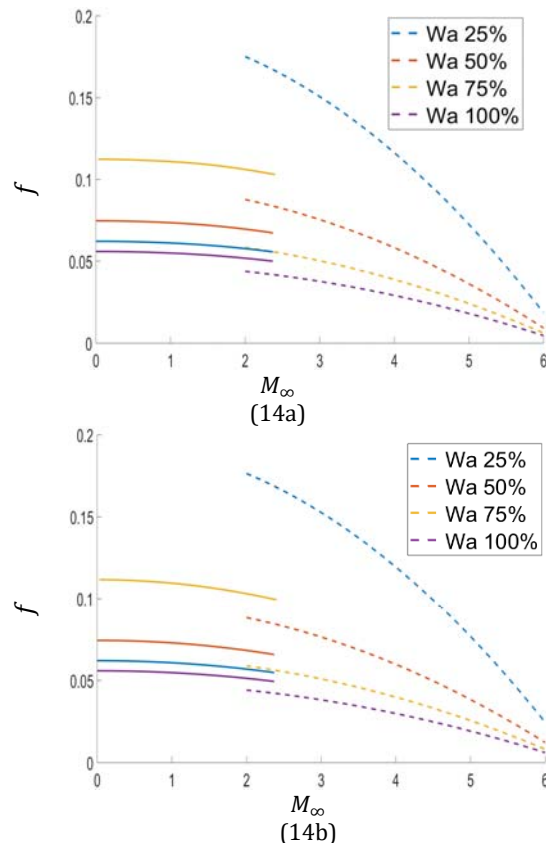


Figure 14. f for variations of inlet air mass flow at 10 km (a) and 20 km (b) for turboramjet engine as a function of M_∞ .

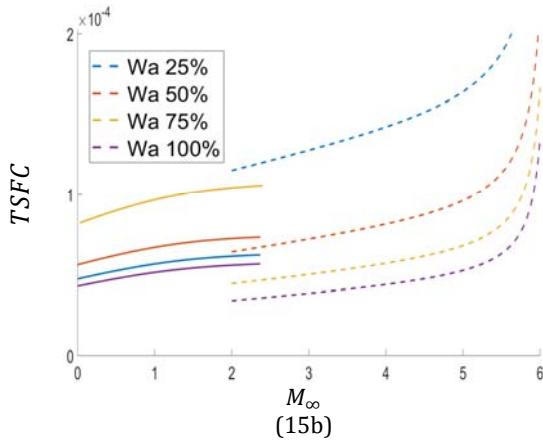
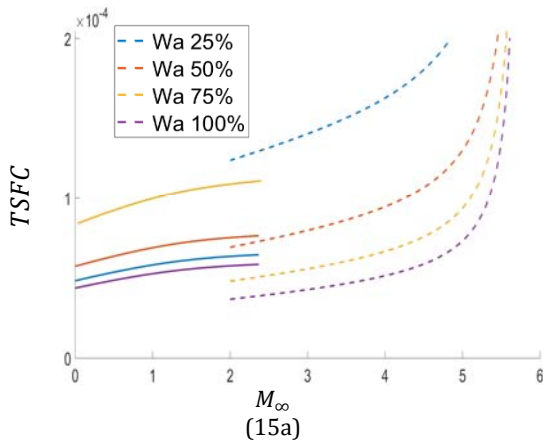


Figure 15. $TSFC$ for variations of inlet air mass flow at 10 km (a) and 20 km (b) for turbojet engine as a function of M_∞ .

Figure 16 also shows that as the inlet air mass flow to either system is increased the I_a (s) decreases. This occurs as a consequence of the specific thrust; whereas the air mass flow increases the specific thrust decreases and therefore, so does the I_a . In general, the ramjet indicates higher attainable I_a at Mach 2 than the turbojet. In addition, the variations of I_a for the turbojet are modest between 10 km and 20 km, whereas the ramjet variations are slightly more pronounced. The turbojet attains specific impulse values of: 95, 90, 88 and 87 versus 96, 91, 90 and 89 at altitudes of 10 km and 20 km respectively. Whereas the ramjet specific impulse values are: 58, 49, 46 and 45 versus 38, 32, 30 and 29 at 10 km and 20 km respectively. However, for a value of 45s and at an altitude of 20 km the ramjet achieves Mach numbers of: 5.07, 4.87, 4.79 and 4.75. Therefore, for the same value of specific impulse, the ramjet is able to reach higher Mach numbers as the altitude increases.

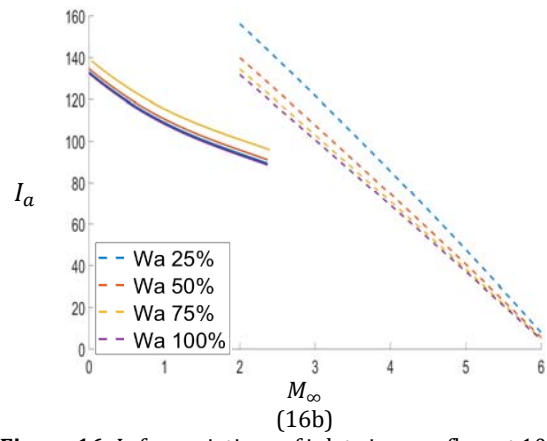
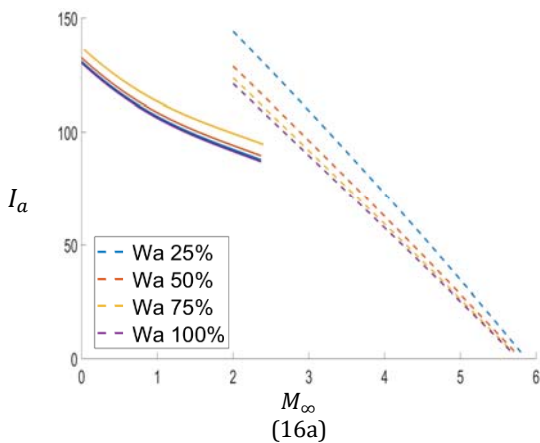


Figure 16. I_a for variations of inlet air mass flow at 10 km (a) and 20 km (b) for turbojet engine as a function of M_∞ .

In general, Figure 17 and Figure 18 illustrate that as the inlet air mass flow is increased to either system, the thrust and power also increases. At a Mach number of 2 the ramjet indicates improved thrust over the turbojet for an inlet mass flow above 25%. However, it is also clearly seen that as the altitude increases from 10 km to 20 km the thrust output decreases from both systems. The turbojet achieves maximum thrust values of: 35, 65, 95 and 126 versus 7, 14, 20 and 27 kN at 10 km and 20 km respectively; a decrease of approximately 4 to 5 fold for an increase in altitude. Whereas the ramjet attains thrust values of: 39, 66, 93 and 120 versus 6, 11, 15 and 19 kN at 10 km and 20 km respectively; a decrease of approximately 6 fold for an increase of altitude. However, the maximum attainable thrust for the ramjet at 10 km are: 50, 88, 126 and 165 at Mach numbers of 3.05, 2.96, 2.99 and 2.92 respectively. Whereas at 20 km the maximum thrust values for the ramjet are: 12, 21, 30 and 39 for Mach number of 3.29, 3.18, 3.16 and 3.12 respectively.

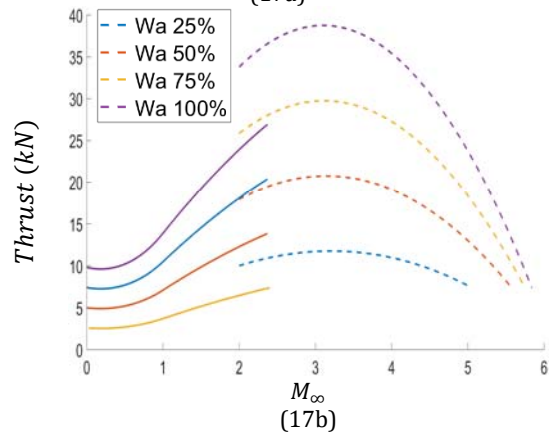
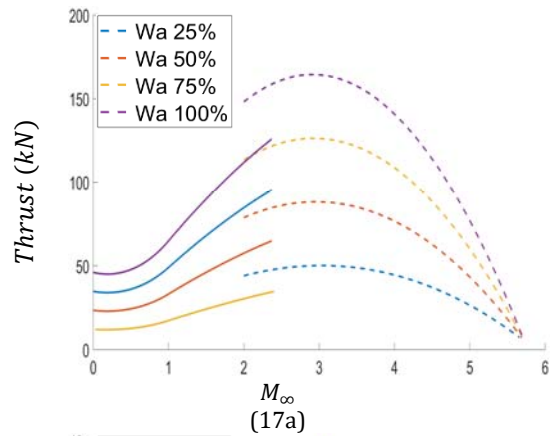


Figure 17. Thrust for variations of inlet air mass flow at 10 km (a) and 20 km (b) for turbojet engine as a function of M_∞ .

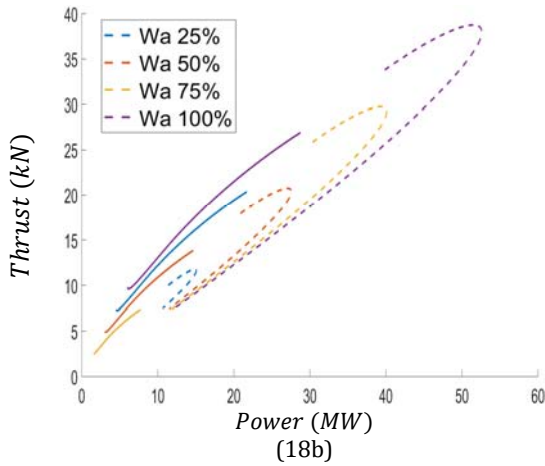
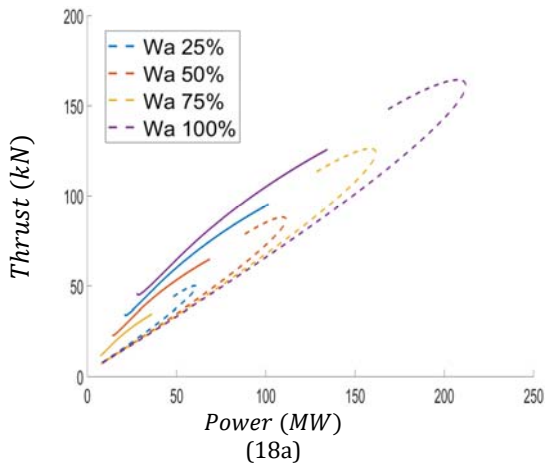


Figure 18. Thrust for variations of inlet air mass flow at 10 km (a) and 20 km (b) for turboramjet engine as a function of Power.

From Figure 19 it can clearly be seen that at all Mach numbers the ramjet is far more advantageous than the turbojet and especially at 20 km. The specific volume of the turbojet at 10 km and 20 km is 10.63 and 51.25 (m^3/kg) respectively; whereas the ramjet values at 10 km and 20 km are 6 and 20 (m^3/kg) respectively. Therefore, the specific volume is 1.7 and 2.4 times larger than that of the ramjet at each altitude respectively; therefore, the trade off in weight is unequivocal. In addition, due to a weak dependency, the variation of inlet air mass flow has very little impact on the specific volume of the exhaust nozzle for both the turbojet and ramjet.

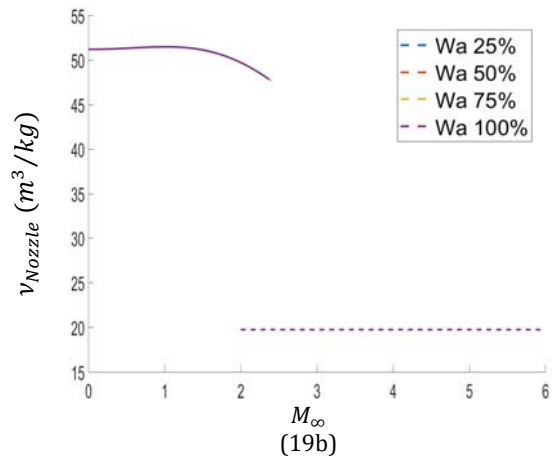
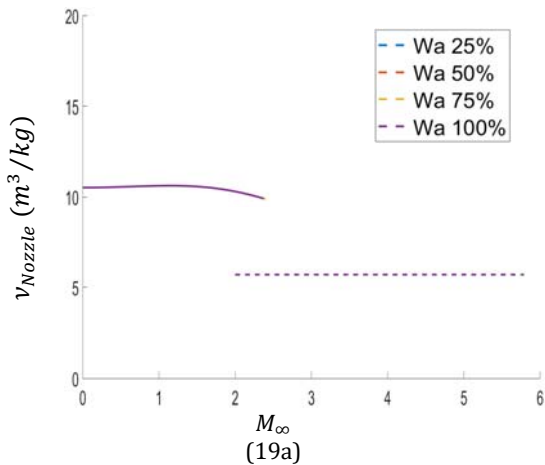


Figure 19. v_{Nozzle} for variations of inlet air mass flow at 10 km (a) and 20 km (b) for turboramjet engine as a function of M_{∞} .

CONCLUSION

This investigation presented two case studies: Case I was a comparison between the Turbojet with and without an AB considering PLOS, EPLOS and maximum power; Case II was an evaluation of a Turboramjet in Dual Mode Operation under maximum power optimization function.

When evaluating Case I, the primary purpose of a turbojet with an AB is to increase thrust, power, specific impulse at the expense of higher fuel consumption, exergy destruction and overall weight of the engine configuration. When evaluating the turbojet with and without an AB from an EPLOS, the variations in Mach number have a very small effect and as the Mach number increase the difference in EPLOS between both engine configuration decreases. PLOS values for both engine configurations indicate a higher exergy destruction for the turbojet with an AB. Nonetheless, at minimum PLOS values the turbojet with an AB can operate at lower θ_c and generate more power than the turbojet without an AB; therefore a decrease in weight is attained as an advantage for the turbojet with an AB. However, a concessional study of a decrease in θ_c and thus compressor weight versus the ~85% increase in exhaust nozzle specific volume and AB fuel components must be conducted. Under maximum power evaluations, the turbojet with an AB has a significant advantage of increase in thrust at all altitudes and Mach numbers, it is only beyond a Mach number of unity does the thermal efficiency of the engine configuration portray higher relevance. On the other hand, it was also seen that for a given altitude, the turbojet with an AB was able to attain the same power and thrust output as the turbojet without an AB at a much lower Mach number. Therefore, when considering lower Mach numbers, the turbojet with AB has a higher advantage in attaining shorter Take-Off distances, especially for military aircrafts on aircraft carriers (i.e. warships). In addition, at higher Mach numbers, the turbojet with an AB has a significantly higher amount of thrust which becomes critical for military type aircrafts in combat mode.

Case II considered the performance evaluation of the turboramjet engine under a maximum power objective function in dual mode operation for variation of altitude and inlet air mass flow split as a function of Mach number. Under dual mode operation the turbojet engine AB were taken to be in the operative state. The results show that the

turbojet operation exhibits a Mach number limitation of 2.51 beyond an altitude of 12 km, whereas the ramjet limitation is in terms of TSFC where beyond a value of 5.694×10^{-5} at a Mach number of 5.26 and altitude of 20 km operation becomes unrealistic. Moreover, as the split of inlet air mass flow to the ramjet was increased beyond 50% the advantage in terms of η_{th} , η_o , f , TSFC, I_a , thrust and v_{NOZZLE} far supersede that of the turbojet with an AB. The ramjet experiences a significant decrease on f for an increase in altitude from 10 km to 20 km and becomes more fuel efficient than the turbojet with an AB at inlet air mass flow splits above 75%. Furthermore, the ramjet is more economical at 20 km than at 10 km operation where for the same value of TSFC a higher Mach number can be attained 5.26 vs. 4.4 however at the expense of lower than maximum thrust. Where maximum thrust for the ramjet occurs at lower Mach number values: 165 kN at 2.92 Mach vs. 39 kN at 3.12 Mach at 10 km and 20 km respectively. Likewise, for the same value of specific impulse (45 s), the ramjet is able to reach higher Mach numbers (4.4 vs. 4.75 at 100% inlet air mass flow split) as the altitude increases, whereas for the turbojet the I_a exhibits minimal change. In addition, the specific volume of the turbojet with an AB is 1.7 and 2.4 times larger than that of the ramjet for an increase in altitude from 10 km to 20 km; therefore, the trade off in weight is indisputable. Moreover, it is seen that the ramjet can commence operation at a Mach number of 2 and begin diverting the inlet mass flow rate from the turbojet with an AB to the ramjet while still remaining competitive with the turbojet with an AB.

REFERENCES

- Şöhret Y., Ekici S. and Karakoç T. H. (2017). Using Exergy for Performance Evaluation of a conceptual Ramjet Engine Burning Hydrogen Fuel, International Journal of Hydrogen Energy, XXX I-6.
<https://doi.org/10.1016/j.ijhydene.2017.12.060>
- Latypov A. F. (2009). Exergy Analysis of Ramjet, Thermophysics and Aeromechanics, Vol. 16, No. 2.
<https://doi.org/10.1134/S0869864309020152>
- Latypov A. F. (2013). Exergy Method for Estimating the Ramjet Specific Impulse, Thermophysics and Aeromechanics, 2013, Vol. 20, No. 5.
<https://doi.org/10.1134/S0869864313050023>
- Ayaz S. K. and Altuntaş Ö. (2017). Assessment of Ramjet Engine for Different Mach Numbers, International Journal of Sustainable Aviation, Vol. 3, No. 4.
<https://doi.org/10.1504/IJSA.2017.090299>
- Moorhouse D. J. (2003). Proposed System-Level Multidisciplinary Analysis Technique Based on Exergy Methods, Journal of Aircraft, Vol. 40, No. 1, January – February.
<https://doi.org/10.2514/2.3088>
- Moorhouse D. J. and Suchomel C. F. (2001). Exergy Method Applied to the Hypersonic Vehicle Challenge, AIAA paper # 2001 – 3063.
- Moorhouse D. J., Hoke C. M. and Prendergast J. P. (2002). Thermal Analysis of Hypersonic Inlet Flow with Exergy-Based Design Methods, International Journal of Thermodynamics, vol. 5 (No. 4), pp. 161-168, December.
- Marley C. D. and Riggins D. W. (2011). The Thermodynamics of Exergy Losses and Thrust Production in Gas Turbine Engines, AIAA, 2011-6130.
- Ispir A. C., Gonçalves P., Kurban E. And Saraçoğlu B. H. (2020). Thermodynamic Efficiency Analysis and Investigation of Exergic Efficiencies of STRATOFly MR3 Aircraft Propulsion Plant, AIAA SciTech Forum, 6-10 January.
- Ehyaei M. A., Anjiridezfuli A. And Rosen M. A. (2013). Exergic Analysis of an Aircraft Turbojet Engine with an Afterburner, Thermal Science, Vol. 17, No. 4, pp 1181-1194.
<https://doi.org/10.2298/TSCI110911043E>
- Roth B. and Marvis D. (2000). A Method for Propulsion Technology Impact Evaluation via Thermodynamic Work Potential, AIAA 2000-4854.
- Camberos J. A. And Moorhouse D. J. (2011). Exergy Analysis and Design Optimization for Aerospace Vehicles and Systems, AIAA, Vol. 238, Progress in Astronautics and Aeronautics.
- Hayes D., Lone M. and Whidborne J. F., Camberos J. and Coetzee E. (2017). Adopting exergy analysis for use in aerospace, Progress in Aerospace Sciences xxx 1–22.
<https://doi.org/10.1016/j.paerosci.2017.07.004>
- Riggins D. W. and Taylor T. (2006). Methodology for Performance Analysis of Aerospace Vehicles Using the Laws of Thermodynamics, JOURNAL OF AIRCRAFT, Vol. 43, No. 4, July–August.
<https://doi.org/10.2514/1.16426>
- Balli Ö. (2017). Advanced exergy analyses to evaluate the performance of a military aircraft turbojet engine (TJE) with afterburner system: Splitting exergy destruction into unavoidable/avoidable and endogenous/exogenous, Applied Thermal Engineering 111 152–169.
<https://doi.org/10.1515/tjj-2016-0074>
- Balli Ö. (2017). Exergetic, Exergoeconomic, Sustainability and Environmental Damage Cost Analyses of J85 Turbojet Engine with Afterburner, International Journal of Turbo & Jet Engines.
<https://doi.org/10.1515/tjj-2017-0019>
- Balli Ö. (2014). Afterburning effect on the energetic and exergetic performance of an experimental turbojet engine (TJE), International Journal of Exergy, January.
<https://doi.org/10.1504/IJEX.2014.060278>
- Akkaya A.V., Şahin B. and Erdem H.H. (2007). Exergetic performance coefficient analysis of a simple fuel cell system, International Journal of Hydrogen Energy 32 4600 – 4609.
<https://doi.org/10.1016/j.ijhydene.2007.03.038>
- Yüksel B., Balli Ö., Günerhan H. and Hepbaşlı A. (2020). Comparative Performance Metric Assessment of a Military Turbojet Engine Utilizing Hydrogen and Kerosene Fuels Through Advanced Exergy Analysis Method, Energies, 13, 1205.
<https://doi.org/10.3390/en13051205>

- Balli Ö., Adak İ. and Güneş S. (2017). Afterburner Effect on the Energetic and Exergetic Performance of J79-GE-17 Engine with Afterburner System used on F-4 Phantom II Aircrafts, International Symposium on Sustainable Aviation (ISSA-2017), Kiev, Ukraine, 10 – 13 September.
- Akkaya A.V., Şahin B. and Erdem H.H. (2008). An analysis of SOFC/GT CHP system based on exergetic performance criteria, International Journal of Hydrogen Energy 33 2566 – 2577. <https://doi.org/10.1016/j.ijhydene.2008.03.013>
- Bastani M., Jafari R. and Ghasemi H. (2015). Exergy Analysis of an Aircraft Turbojet Engine, International Journal of Engineering Sciences & Research Technology, ISSN: 2277-9655, April.
- Yüksel B., Günerhan H. and Hepbaşlı A. (2020). Assessing Exergy-Based Economic and Sustainability Analyses of a Military Gas Turbine Engine Fueled with Various Fuels, Energies, 13, 3823. <https://doi.org/10.3390/en13153823>
- Niknamian S. (2020). The optimization of a jet turbojet engine by PSO and searching algorithms, Social Science Research Network, <https://ssrn.com/abstract=3503740>, January. <https://doi.org/10.35877/454RI.asci3195>
- Sürer M.G. and Arat H.T. (2018). A Critical Review of Exergy Studies on Jet Engines, 16th International Conference on Clean Energy (ICCE-2018), May.
- Dong Z., Li D., Wang Z. and Sun M. (2018). A Review on Exergy Analysis of Aerospace Power Systems, Acta Astronautica, AA 7090, S0094-5765(18)31012-9, September. <https://doi.org/10.1016/j.actaastro.2018.09.003>
- Noori F., Gorji M., Kazemi A. and Nemati H. (2015). Thermodynamic optimization of ideal turbojet with afterburner engines using non-dominated sorting genetic algorithm II, Journal of Aerospace Engineering, Proc. IMechE Vol. 224 Part G, February. <https://doi.org/10.1243/09544100JAERO771>
- Nasab M.R.A. and Ehyaei M.A. (2019). Optimization of turbojet engine cycle with dual-purpose PSO algorithm, Mechanics & Industry 20, 604, March. <https://doi.org/10.1051/meca/2019029>
- Liu, Y., Mo, D. and Wu, Y. (2023). Design of Hypersonic Variable Cycle Turboramjet Engine Based on Hydrogen Fuel Aiming at 2060 Carbon Neutralization. The Proceedings of the 2021 Asia-Pacific International Symposium on Aerospace Technology (APISAT 2021), Volume 2. APISAT 2021. Lecture Notes in Electrical Engineering, vol 913. Springer, Singapore. https://doi.org/10.1007/978-981-19-2635-8_85
- Rajashankar S., Ananthkrishnan N., Sharma A., Lee J. and Namkoug H.J. (2024). Turbojet Module Sizing for Integration with Turbine-Based Combined Cycle Engine, Cornell University, Physics, Fluid Dynamics, arXiv:2406.19472v1 [physics.flu-dyn] 27 Jun 2024. <https://doi.org/10.48550/arXiv.2406.19472>
- Xi Z., Zhang H., Chen M., Cai C. and Wang J. (2023). Design of thrust augmentation control schedule during mode transition for turbo-ramjet engine, Aerospace Science and Technology Volume 138, July 2023, 108352 <https://doi.org/10.1016/j.ast.2023.108352>
- Lockheed Martin SR-72, "Son of Blackbird" (2024). https://en.m.wikipedia.org/wiki/Lockheed_Martin_SR-72 <https://www.youtube.com/watch?v=vFMIQOMaUXI>
- Fawal S. and Kodal A. (2019). Comparative performance analysis of various optimization functions for an irreversible Brayton cycle applicable to turbojet engines, Energy Conversion and Management, 199 111976. <https://doi.org/10.1016/j.enconman.2019.111976>
- Fawal S. and Kodal A. (2021). Overall and Component Basis Performance Evaluations for Turbojet Engines Under Various Optimal Operating Conditions, Aerospace Science and Technology 117 106943. <https://doi.org/10.1016/j.ast.2021.106943>
- MIL-E-5007D (1973). General Specification for Engines, Aircraft, Turbojet and Turbofan, Military Specification, Department of the Air Force, Wright-Paterson AFB, OH, September.
- Keith T.G. and John J.E. (2006). Gas Dynamics, Third Edition, Pearson, Prentice Hall, Upper Saddle River, NJ.
- El-Sayed A.F. (2016). Fundamentals of Aircraft and Rocket propulsion, Department of Mechanical Engineering, Zagazig University, Zagazig, Egypt, Springer-Verlag London.
- Mattingly J. D. (1996). Elements of Gas Turbine Propulsion, TATA McGraw-Hill Edition.
- Farokhi S. (2014). Aircraft Propulsion, 2nd Edition, Wiley.